Iterative defect correction and multigrid accelerated explicit time stepping for the steady Euler equations

Barry Koren

CWI, Amsterdam, The Netherlands

Marie-Hélène Lallemand

INRIA, France

1 Introduction

1.1 Equations

The equations considered are the steady, 2D, compressible Euler equations

$$\frac{\partial F(W)}{\partial x} + \frac{\partial G(W)}{\partial y} = 0, \tag{1.1}$$

where

$$W = \begin{pmatrix} \rho \\ \rho u \\ \rho v \\ \rho e \end{pmatrix}, \tag{1.2a}$$

$$F(W) = \begin{pmatrix} \rho u \\ \rho u^2 + p \\ \rho u v \\ \rho u(e + \frac{p}{\rho}) \end{pmatrix}, \quad G(W) = \begin{pmatrix} \rho v \\ \rho v u \\ \rho v^2 + p \\ \rho v(e + \frac{p}{\rho}) \end{pmatrix}. \tag{1.2b}$$

Assuming a perfect gas, the total energy e satisfies: $e = \frac{1}{\gamma-1}\frac{p}{\rho} + \frac{1}{2}(u^2 + v^2)$. The ratio of specific heats γ is assumed to be constant.

1.2 Spatial discretization

The computational grid is obtained by a hybrid finite element - finite volume partition. A (possibly unstructured) finite-element triangularization is used as the basic partition. A cell-centered finite-volume partition is derived from the finite-element partition by connecting the centers of the triangle sides in the manner illustrated in Figure 1. The finite-volume grid gives us the easy possibility of grouping together the nodes associated with contiguous finite volumes. If we take unions of control volumes this re-
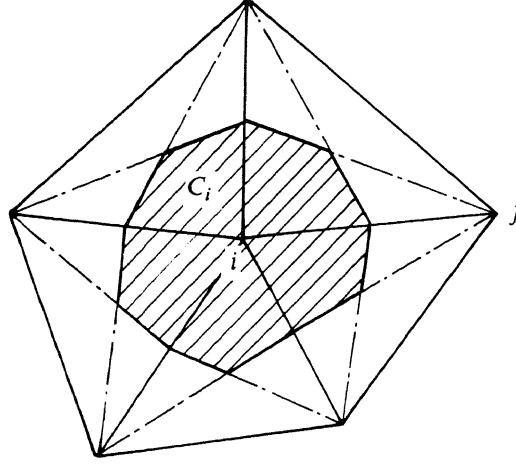
FIG. 1. Finite volume C_i

Euler and Navier-Stokes flow computations, we refer to Dervieux *et al.* (1989), and Rostand and Stoufflet (1989), respectively. For details about the coarsening process (multilevel gridding) we refer to Lallemand and Dervieux (1988).

On the finest grid, for all finite volumes C_i, $i = 1, 2, \ldots, N$, we consider the integral form

$$\oint_{\partial C_i} (F(W)n_x + G(W)n_y)\,ds = 0, \quad i = 1, 2, \ldots, N, \qquad (1.3)$$

with n_x and n_y the x- and y-component of the outward unit normal on the volume boundary ∂C_i. For the Euler equations, because of their rotational invariance, (1.3) may be rewritten as

$$\oint_{\partial C_i} T^{-1}(n_x, n_y)F(T(n_x, n_y)W)ds = 0, \quad i = 1, 2, \ldots, N, \qquad (1.4)$$

where $T(n_x, n_y)$ is the rotation matrix

$$T(n_x, n_y) = \begin{pmatrix} 1 & 0 & 0 & 0 \\ 0 & n_x & n_y & 0 \\ 0 & -n_y & n_x & 0 \\ 0 & 0 & 0 & 1 \end{pmatrix}. \qquad (1.5)$$

For simplicity, we assume the flux to be constant across each bi-segment ∂C_{ij} of the boundary ∂C_i, where $\partial C_{ij} = \partial C_i \cap \partial C_j$ is the common

a. Bi-segment ∂C_{ij} b. Straight segment δC_{ij}
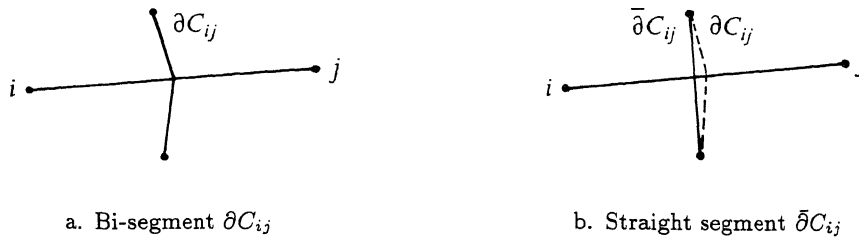
FIG. 2. Segments in between finite volumes C_i and C_j

boundary between the neighboring volumes C_i and C_j (Figure 2a). Hence, $\partial C_i = \cup \partial C_{ij}$, $j = 1, 2, \ldots, n_i$, with n_i the number of neighboring volumes C_j. (In the example of Figure 1: $n_i = 5$.) Since we have assumed that the flux is constant along ∂C_{ij}, it is equal to the flux across the straight segment δC_{ij} connecting the two extreme points of ∂C_{ij} (Figure 2b). If we introduce the outward unit normal $\bar{n}_{ij} = ((\bar{n}_x)_{ij}, (\bar{n}_y)_{ij})^T$ along each δC_{ij}, $j = 1, 2, \ldots, n_i$, with the assumption of a constant flux, the contour integral (1.4) can be rewritten as the sum

$$\sum_{j=1}^{n_i} \bar{T}_{ij}^{-1} F(\bar{T}_{ij} W_{ij}) l_{ij} = 0, \quad i = 1, 2, \ldots, N, \tag{1.6}$$

where $\bar{T}_{ij} = T((\bar{n}_x)_{ij}, (\bar{n}_y)_{ij})$, where W_{ij} is some value of W depending on for instance W_i and W_j, and where l_{ij} is the length of the segment δC_{ij}.

Crucial in (1.6) is the way in which the cell-face flux $F(\bar{T}_{ij} W_{ij})$ is evaluated. For this we use an upwind scheme which follows the Godunov principle (Godunov 1959), which assumes that the constant flux vector along each segment δC_{ij} is determined only by a uniformly constant left and right cell-face state (W_{ij}^l and W_{ij}^r). The 1D Riemann problem which then arises at each cell face is solved in an approximate way. With this, (1.6) can be further rewritten as

$$\sum_{j=1}^{n_i} \bar{T}_{ij}^{-1} \Phi(\bar{T}_{ij} W_{ij}^l, \bar{T}_{ij} W_{ij}^r) l_{ij} = 0, \quad i = 1, 2, \ldots, N, \tag{1.7}$$

where Φ denotes the approximate Riemann solver. Several approximate Riemann solvers exist; see for example Roe (1981), and Osher and Solomon (1982). In the present paper - without any particular motivation - we restrict ourselves to the application of the approximate Riemann solver of Osher and Solomon (1982).

The flux evaluation, and so the space discretization, may be either first-or higher-order accurate. First-order accuracy is obtained in the standard way; at each finite-volume wall, the left and right cell-face state which have to be inserted in the numerical flux function are taken equal to those in the corresponding adjacent volumes:

$$W_{ij}^l = W_i, \quad W_{ij}^r = W_j. \tag{1.8}$$

Whereas the first-order accurate discretization is applied at all levels, the higher-order discretization is applied at the finest grid only, using the finite-element partition existing there. Higher-order accuracy is obtained with a MUSCL-approach (Van Leer 1979). Here, W_{ij}^l and W_{ij}^r are derived from linear interpolations. On each volume C_i around the triangle-vertex i an approximate gradient, denoted by $(\bar{\nabla}W)_i$, is derived by integrating the gradient of the linear interpolant of W over all the triangles which have i as a vertex:

$$(\bar{\nabla}W)_i = \left(\left(\frac{\bar{\partial}W}{\partial x}\right)_i, \left(\frac{\bar{\partial}W}{\partial y}\right)_i \right)^T, \quad \text{with} \tag{1.9a}$$

$$\left(\frac{\bar{\partial}W}{\partial x}\right)_i = \frac{\int_{\text{supp}(i)} \frac{\partial W}{\partial x} dx\, dy}{\int_{\text{supp}(i)} dx\, dy}, \quad \left(\frac{\bar{\partial}W}{\partial y}\right)_i = \frac{\int_{\text{supp}(i)} \frac{\partial W}{\partial y} dx\, dy}{\int_{\text{supp}(i)} dx\, dy}. \tag{1.9b}$$

In here, supp(i) denotes the union of triangles which have i as a vertex. Then for each pair of neighboring vertices (i, j) we compute the extrapolated values

$$W_{ij}^l = W_i + \frac{1}{2}(\bar{\nabla}W)_i \cdot \vec{ij}, \quad W_{ij}^r = W_j - \frac{1}{2}(\bar{\nabla}W)_j \cdot \vec{ij}. \tag{1.10}$$

On equidistant grids, this higher-order accurate discretization can be formally proved to be second-order accurate. The proof is still valid for nearly equidistant grids. In the present paper we do not analyze orders of accuracy; the discretization is already known. It has been described in more detail in various other papers; see for example Fézoui and Stoufflet (1989). In order to ensure monotonicity, while preserving the higher-order accuracy in smooth flow regions, the higher-order values W_{ij}^l and W_{ij}^r according to (1.10) can be replaced by limited values which do not affect the order of accuracy.

1.3 Existing solution method

To solve the steady discretized system (1.7), we consider the unsteady, semi-discrete system of ordinary differential equations

$$\frac{dW_i}{dt} = R_i, \quad i = 1, 2, \ldots, N. \tag{1.11}$$

The natural choice for R_i is

$$R_i = \frac{-1}{A_i} \sum_{j=1}^{n_i} \bar{T}_{ij}^{-1} \Phi(\bar{T}_{ij} W_{ij}^l, \bar{T}_{ij} W_{ij}^r) l_{ij}, \qquad (1.12)$$

where A_i is the area of finite volume C_i.

As an upwind analogue to Jameson's central method (Jameson 1983), in Lallemand and Dervieux (1988), and Lallemand (1990) an explicit four-stage Runge-Kutta (RK4-) scheme is applied for the temporal integration of (1.11)-(1.12). The benefits of the upwind analogue are evident: better shock capturing, greater robustness and no tuning of explicitly added artificial viscosity. Similarly, just as in Jameson (1983), in Lallemand and Dervieux (1988) multigrid is applied for accelerating the solution process. Furthermore, just as in Jameson (1983), time accuracy is not pursued and optimal Runge-Kutta coefficients are applied to get good stability as well as good smoothing properties. It seems that the solution method presented in Lallemand and Dervieux (1988) is already competitive with Jameson's method, without the introduction of a further acceleration technique such as for example residual averaging.

It is of interest that the upwind analogue allows a further efficiency improvement by exploitation of the direct availability of the corresponding first-order upwind discretization, with its better stability and smoothing properties. Since a first-order central discretization is not readily available, a standard central method does not easily allow this improvement.

2 Novel solution method

2.1 Explicit time stepping

Compared with the existing solution method, the new solution method only uses a more extensive right-hand side in the explicit time-stepping scheme. The extension consists of two first-order upwind defects, one which is evaluated at each stage of the multistage scheme, and another which is kept frozen during a fixed number of ν_t RK4-time-steps ($\nu_t \geq 1$) and which compensates for the other first-order defect by its opposite sign. Further - which is important - the higher-order defect is kept frozen as well during ν_t RK4-steps. The four-stage time-stepping scheme is given in Table 1. In here, ν is the time-step number, k the stage number, Δt_i the local time step and α_k the k-th Runge-Kutta coefficient. In the existing higher-order method the right-hand side $R_i^{\nu,k-1}$ is

$$R_i^{\nu,k-1} = \frac{-1}{A_i} \sum_{j=1}^{n_i} \bar{T}_{ij}^{-1} \Phi(\bar{T}_{ij} (W_{ij}^l)^{\nu,k-1}, \bar{T}_{ij} (W_{ij}^r)^{\nu,k-1}) l_{ij}, \qquad (2.1)$$

with $(W_{ij}^l)^{\nu,k-1}$ and $(W_{ij}^r)^{\nu,k-1}$ higher-order accurate. So nothing is kept frozen in the existing method's right-hand side. For the novel method we

Table 1 Explicit RK4-scheme

$W_i^{0,4} := W_i^{0,0}, \quad i = 1, 2, \ldots, N$

for ν **from** 1 **to** ν_t **do**

$\quad W_i^{\nu,0} := W_i^{\nu-1,4}, \quad i = 1, 2, \ldots, N$

$\quad$ **for** k **from** 1 **to** 4 **do**

$\quad\quad W_i^{\nu,k} := W_i^{\nu,0} + \Delta t_i \, \alpha_k \, R_i^{\nu,k-1}, \quad i = 1, 2, \ldots, N$

$\quad$ **enddo**

enddo

---

take

$$R_i^{\nu,k-1} = \frac{-1}{A_i} \sum_{j=1}^{n_i} \bar{T}_{ij}^{-1} \left[\Phi(\bar{T}_{ij} W_i^{\nu,k-1}, \bar{T}_{ij} W_j^{\nu,k-1}) - \right.$$

$$\Phi(\bar{T}_{ij} W_i^{0,0}, \bar{T}_{ij} W_j^{0,0}) +$$

$$\left. \Phi(\bar{T}_{ij} (W_{ij}^l)^{0,0}, \bar{T}_{ij} (W_{ij}^r)^{0,0}) \right] l_{ij}, \qquad (2.2)$$

where only $(W_{ij}^l)^{0,0}$ and $(W_{ij}^r)^{0,0}$ are higher-order accurate. The frozen first-order cell-face states $(W_i^{0,0}$ and $W_j^{0,0})$ and the frozen higher-order cell-face states $((W_{ij}^l)^{0,0}$ and $(W_{ij}^r)^{0,0})$ are updated in an additional outer iteration, which will be explained in the next section. In the following, for convenience, $W^{\nu,4}$ will also be denoted as $W_{\text{RK4}}(\nu, R^{0,0}, W^{0,0})$.

2.2 Complete solution method

The novel solution method is of defect correction type (Böhmer *et al.* 1984). Though defect correction iteration is not as necessary for a pseudo-unsteady solution method as it is for a solution method which directly tackles steady discretized equations (Hemker 1986, Koren 1988 and Koren 1990), it may lead to an improved efficiency.

The new solution method can be divided into two successive stages. The first stage is *nested iteration* (Hackbusch 1985, p.98), also called *full multigrid (FMG)* method (Brandt 1982), which is applied to obtain a good initial solution on the finest grid. The second stage is an *iterative defect correction (IDeC)* method (Böhmer *et al.* 1984 and Hackbusch 1985, p.282), which is used to iterate until the higher-order accurate solution is obtained. The initial solution for the defect correction process is the solution obtained by the nested iteration. The inner iteration of both stages is a *nonlinear multigrid* method (Hackbusch 1985, p.181), viz. the *full approximation storage (FAS)* algorithm (Brandt 1977 and Brandt 1982). In the following sections we discuss successively: the nested iteration (Section 2.2.1), the iterative defect correction method (Section 2.2.2), and the building block of these two iterations: the nonlinear multigrid iteration (Section 2.2.3).

2.2.1 Nested iteration

To apply multigrid we construct a nested set of grids. Let $\Omega_1, \Omega_2, \ldots, \Omega_L$ be a sequence of nested grids with Ω_1 the coarsest and Ω_L the finest grid. (For a description of the coarsening rule applied here, we refer to Lallemand and Dervieux (1988).) The nested iteration (FMG) starts with a user-defined initial estimate of W_1: the solution on the coarsest grid Ω_1. To obtain an initial solution on Ω_2, the solution on Ω_1 is first improved by a few FAS-cycles. (The number of FAS-cycles which is applied in each FMG-step can be either fixed, $\nu_{\text{FAS}} = $ constant, or dependent on the residual.) After this, the improved solution W_1 is prolongated to Ω_2. The process is repeated until Ω_L has been reached.

The prolongation of the solution can be the simple piecewise constant prolongation I_{l-1}^l, $2 \leq l \leq L$, or it can be a smoother one. If we denote the area of finite volume C_i^l at level l by A_i^l, and the number of neighboring volumes C_j^l of C_i^l by n_i^l, a smooth prolongation operator $\mathcal{I}_{l-1}^l$ is defined by

$$(\mathcal{I}_{l-1}^l(W_{l-1}))_i \equiv \frac{A_i^l (I_{l-1}^l(W_{l-1}))_i + \sum_{j=1}^{n_i^l} A_j^l (I_{l-1}^l(W_{l-1}))_j}{A_i^l + \sum_{j=1}^{n_i^l} A_j^l}, \quad 2 \leq l \leq L.$$

(2.3)

We notice that since I_{l-1}^l strictly obeys the physical conservation laws by the prolongation of cell-integrated amounts of mass, momentum and energy, $\mathcal{I}_{l-1}^l$ is strictly conservative as well.

2.2.2 Iterative defect correction

Let $\mathcal{F}_L^1(W_L) = 0$ and $\mathcal{F}_L^+(W_L) = 0$ denote the first-order and higher-order discretized Euler equations, respectively, on the finest grid. Then, IDeC can be written as

$$\mathcal{F}_L^1(W_L^0) = 0,$$

(2.4a)

$$\mathcal{F}_L^1(W_L^n) = \mathcal{F}_L^1(W_L^{n-1}) - \mathcal{F}_L^+(W_L^{n-1}), \quad n = 1, 2, \ldots, n_{\text{IDeC}},$$

(2.4b)

where W_L^0 is the solution yielded by FMG. ¿From (2.4b), it is immediately clear that at convergence $(W_L^n = W_L^{n-1} = W_L)$, we have solved the higher-order discretized Euler equations $\mathcal{F}_L^+(W_L) = 0$. Therefore, we emphasize that the present defect correction method is *not* mixed defect correction iteration (Hemker 1984). (A mixed defect correction method would yield a solution whose accuracy is not well-defined; its solution would be a vague mixture of the first-order and higher-order accurate solutions.) Though both theory (Désidéri and Hemker 1990) and practice (Désidéri and Hemker 1990) show that IDeC gives poor convergence of the residual, theory (Hackbusch 1981 and Hackbusch 1985, p.282) and practice (Hemker 1986 and Koren 1990) also show that for smooth problems, a single IDeC-cycle ($n_{\text{IDeC}} = 1$) is sufficient to obtain second-order solution accuracy. Further, for solutions with discontinuities, a few IDeC-cycles ($n_{\text{IDeC}} \approx 5$)

may improve the accuracy to a sufficient extent (Hemker 1986 and Koren 1988). In summary: for both smooth and non-smooth flow problems, numerical experiments with IDeC show this phenomenon of *slow convergence* but of *fast solution improvement* (Hemker 1986, Koren 1988, Koren 1990, and Désidéri and Hemker 1990); a phenomenon which is understood by theory (Hackbusch 1981, Hackbusch 1985, p.282, and Désidéri and Hemker 1990).

In each IDeC-cycle we have to solve a first-order system with an appropriate right-hand side. From Koren (1988) it is known that it is inefficient to solve this system very accurately. With a steady approach, application of only a single FAS-cycle per IDeC-cycle appears to be the most efficient strategy in Koren (1988). In the present paper, with our unsteady approach, we will re-investigate what is the most efficient number of FAS-cycles per IDeC-cycle (see Section 3).

2.2.3 *Nonlinear multigrid iteration*

Let us denote by $(W_l)_{V(\nu_{\mathrm{pre}}, \nu_{\mathrm{post}})}(\nu_{\mathrm{FAS}}, R_l, W_l^0)$ the solution obtained on level l, after ν_{FAS} FAS-V$(\nu_{\mathrm{pre}}, \nu_{\mathrm{post}})$-cycles have been applied to $\mathcal{F}_l^1(W_l) = R_l$, with initial solution W_l^0. A single FAS-V$(\nu_{\mathrm{pre}}, \nu_{\mathrm{post}})$-cycle on level l, $1 \leq l \leq L$, is then recursively defined by the following successive steps:

1. Improve on the grid Ω_l the initial solution W_l^0 by applying ν_{pre} RK4-steps to

$$\mathcal{F}_l^1(W_l) = R_l. \tag{2.5}$$

Let us denote the resulting solution $(W_l)_{\mathrm{RK4}}(\nu_{\mathrm{pre}}, R_l, W_l^0)$ by $\bar{W}_l$.

2. Coarse-grid correction step: Approximate on the underlying coarser grid Ω_{l-1} the solution of

$$\mathcal{F}_{l-1}^1(W_{l-1}) = R_{l-1}, \tag{2.6a}$$

$$R_{l-1} = \mathcal{F}_{l-1}^1(I_l^{l-1}(\bar{W}_l)) - \tilde{I}_l^{l-1}(\mathcal{F}_l^1(\bar{W}_l) - R_l), \tag{2.6b}$$

by applying a single FAS-V$(\nu_{\mathrm{pre}}, \nu_{\mathrm{post}})$-cycle on level $l - 1$. Let us denote the resulting approximate solution $(W_{l-1})_{V(\nu_{\mathrm{pre}}, \nu_{\mathrm{post}})}(1, R_{l-1}, I_l^{l-1}(\bar{W}_l))$ by $\bar{W}_{l-1}$.

3. Improve the solution on Ω_l by first correcting the approximate solution $\bar{W}_l$ obtained in step (1):

$$\bar{W}_l := \bar{W}_l + I_{l-1}^l(\Delta W_{l-1}), \tag{2.7}$$

where $\Delta W_{l-1} = \bar{W}_{l-1} - I_l^{l-1}\bar{W}_l$ is the result of the coarse-grid correction step (2). Further improve $\bar{W}_l$ by applying ν_{post} RK4-steps to (2.5): $W_l := (W_l)_{\mathrm{RK4}}(\nu_{\mathrm{post}}, R_l, \bar{W}_l)$.

In the FMG-stage, in step (1), we have on each starting (locally finest) grid Ω_l, $1 \leq l \leq L$: $R_l = 0$. Hence, the initial solution for IDeC as

a. $L = 2$, $\nu_{\text{pre}} = 1$, $\nu_{\text{post}} = 2$, $\nu_{\text{FAS}} = 2$, $n_{\text{IDeC}} = 2$

b. $L = 3$, $\nu_{\text{pre}} = \nu_{\text{post}} = 1$, $\nu_{\text{FAS}} = 1$, $n_{\text{IDeC}} = 3$
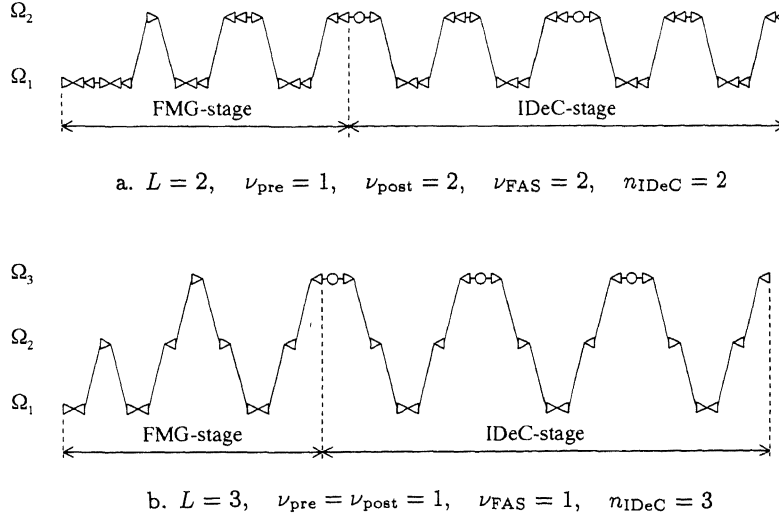
FIG. 3. Examples of complete solution schedule

obtained by FMG is at most first-order accurate. In the IDeC-stage the starting grid is always the globally finest grid Ω_L, and there we have: $R_L = \mathcal{F}_L^1(W_L) - \mathcal{F}_L^+(W_L)$. This higher-order right-hand side is kept frozen during ν_{FAS} FAS-V($\nu_{\text{pre}}, \nu_{\text{post}}$)-cycles per IDeC-cycle. Notice that with the novel method we evaluate the higher-order operator at most once per FAS-V($\nu_{\text{pre}}, \nu_{\text{post}}$)-cycle, instead of $4 \times (\nu_{\text{pre}} + \nu_{\text{post}}) + 1$ times per FAS-V($\nu_{\text{pre}}, \nu_{\text{post}}$)-cycle with the existing method.

In step (2), notice that in the RK4-scheme, the complete right-hand side R_{l-1} is kept frozen. Just as the prolongation operator I_{l-1}^l, the restriction operator I_l^{l-1} is such that it also exactly obeys the conservation of cell-integrated mass, momentum and energy. The restriction operator $\tilde{I}_l^{l-1}$ restricts the defect in the standard way: by summation of mass, momentum and energy defects over fine-grid cells whose union is a coarse cell. On the coarsest grid (Ω_1), step (2) (the coarse-grid correction step) is skipped of course.

To illustrate the structure of the complete novel solution method, we give two examples of a complete higher-order solution schedule in Figure 3. The schedule in Figure 3a is fixed by: $L = 2$, $\nu_{\text{pre}} = 1$, $\nu_{\text{post}} = 2$, $\nu_{\text{FAS}} = 2$, $n_{\text{IDeC}} = 2$. The schedule in Figure 3b is fixed by: $L = 3$, $\nu_{\text{pre}} = \nu_{\text{post}} = 1$, $\nu_{\text{FAS}} = 1$, $n_{\text{IDeC}} = 3$. In both figures, the marker $\triangleright$ denotes a single RK4-step (over Ω_l) preceding a coarse-grid correction, whereas the marker $\triangleleft$ denotes a single RK4-step after the coarse-grid correction. The marker $\bigcirc$ denotes the computation of $R_L =$

$\mathcal{F}_L^1(W_L) - \mathcal{F}_L^+(W_L)$. Notice that the corresponding first-order variants of both schedules (i.e. the variants without any marker $\bigcirc$) are simply obtained by taking $n_{\mathrm{IDeC}} = 0$.

3 Numerical results

In Lallemand and Koren (submitted), by analysis we found that the new higher-order method has better stability and smoothing properties than the existing higher-order method. In order to verify these predicted better stability and convergence properties, we compute the standard transonic channel flow from Rizzi and Viviand (1981) with the 2D Euler equations. Three finest grids are considered: a 161-vertices grid, an about twice as fine 585-vertices grid and an about four times as fine 2225-vertices grid. (See Lallemand and Dervieux (1988) for more grid details.) The corresponding solution schedules applied are a 4-, 5- and 6-levels schedule ($L = 4, 5, 6$), respectively, all with $\nu_{\mathrm{pre}} = \nu_{\mathrm{post}} = 1, \forall l$.

In Figure 4a we present various convergence histories as obtained for $L = 4, 5, 6$, respectively. The convergence results presented are:

- those of the first-order discretized Euler equations solved by means of the nonlinear multigrid iteration (dotted lines),

- those of higher-order discretized Euler equations solved by means of the existing higher-order method (dashed lines), and

- those of higher-order discretized Euler equations solved by means of the novel higher-order method (solid lines).

In all three graphs in Figure 4a, the residual considered is the L_2-norm of the error in the conservation of mass over all the finest-grid cells. Further, in all three graphs, the number of cycles indicated along the horizontal axis is:

- the number of FAS-cycles in case of both the first-order method and the existing higher-order method, and

- the number of IDeC-cycles in case of the new higher-order method.

Note that with the new higher-order method, for $\nu_{\mathrm{FAS}} = 2, 5, 10$ the number of inner FAS-cycles is respectively 2, 5 and 10 times larger than the number of indicated IDeC-cycles. (Only for $\nu_{\mathrm{FAS}} = 1$, the number of FAS-cycles equals the number of IDeC-cycles.) All convergence histories start at the end of the FMG-stage (Figure 3). In agreement with the theoretical results presented in Lallemand and Koren (submitted), for all four values of ν_{FAS} (so also for $\nu_{\mathrm{FAS}} = 1$), the new method does indeed give a better convergence than the existing higher-order method. For decreasing mesh width, the convergence of the new higher-order method becomes even relatively better than that of the first-order method. (For all four values of ν_{FAS} under consideration, the corresponding convergence histories in Figure 4a show a better grid-independency than those of the multigrid method
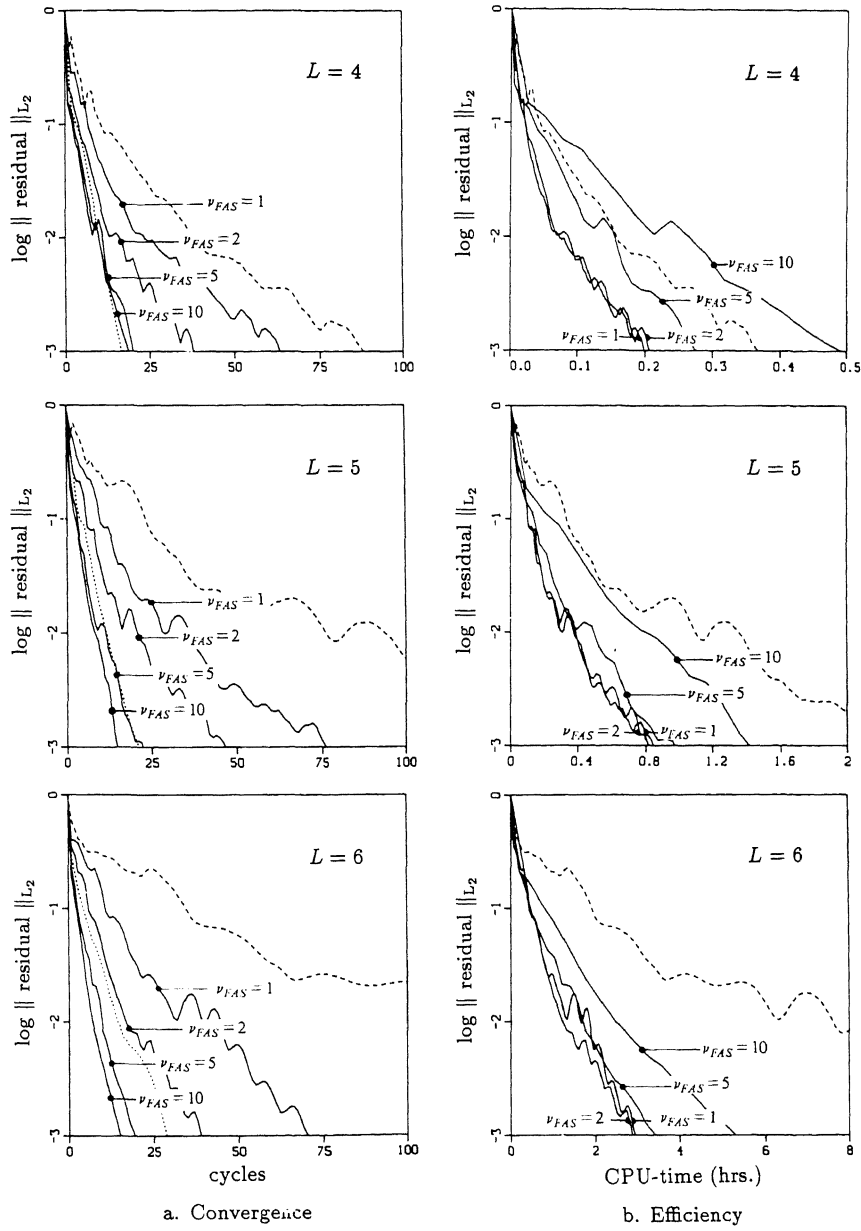
a. Convergence   b. Efficiency

FIG. 4. Convergence and efficiency histories (first-order method: ···, existing higher-order method: ———, novel higher-order method: —)

applied to the first-order discretized equations.) This better performance is probably due to the predicted better smoothing in the new method.

As for the actual order of accuracy, if we took the converged higher-order accurate solution obtained on the 2225-vertices grid as the reference solution, we measured local orders of accuracy in the range $[O(h^{1.4}), O(h^{2.3})]$ for the solutions on the coarser grids (the 585-vertices grid and the 161-vertices grid). The global order of accuracy appears to be almost $O(h^2)$.

Finally, the important question still remains which of the various higher-order methods is the most efficient. To answer this question, we give the higher-order efficiency histories in Figure 4b. The indicated computing times have been obtained on a Sequent. (No efforts have been undertaken to make efficient use of the parallelization features of the machine. What interests us here, is the relative efficiency of the higher-order methods only.) Since the sizes of the three grids considered are related to each other by approximately a factor 4, we have related the scales along the horizontal axes accordingly. Concerning the relative efficiency of the novel higher-order method, for the four values of ν_{FAS} considered, it appears that for all three grids the best efficiency is obtained with $\nu_{\text{FAS}} = 1$ (so just as in Koren (1988), for the schedule with only a single FAS-cycle per IDeC-cycle.) Further it appears - and this is important - that the novel method with $\nu_{\text{FAS}} = 1$ is also more efficient than the existing higher-order method. Due to the better grid-independency of the novel method, this relatively better efficiency becomes even increasingly better with decreasing mesh width.

4 Conclusions

Fully implicit solution methods for higher-order discretized equations may strongly benefit from iterative defect correction when these systems of discretized equations are not easily invertible, which often is the case with higher-order accurate discretizations. Fully explicit solution methods may also profit from iterative defect correction. Here the profits are faster convergence and higher efficiency. The defect correction method appears to lead to greater stability (and hence to greater robustness) than the existing (standard) explicit method. Compared to the existing explicit method it possesses remarkably good smoothing properties, in fact even better than the first-order method. Last but not least its convergence rate appears to be grid-independent. For upwind discretizations, the 'price' which has to be paid for using defect correction iteration - a slightly more complex algorithm - is negligible, because of the direct availability of an appropriate approximate operator: the first-order upwind operator.

Acknowledgements

References

[1] Baba, K. and Tabata, M. (1981). On a conservative upwind finite element scheme for convective diffusion equations, *RAIRO Numer. Anal.*, *15*, 3-25.

[2] Böhmer, K., Hemker, P.W. and Stetter, H.J. (1984). The defect correction approach, *Computing Suppl.*, *5*, 1-32.

[3] Brandt, A. (1977). Multi-level adaptive solutions to boundary-value problems, *Math. Comput.*, *31*, 330-399.

[4] Brandt, A. (1982). Guide to multigrid development, *Lecture Notes in Mathematics*, *960*, 220-312. Springer, Berlin.

[5] Dervieux, A., Désidéri, J.-A., Fézoui, F., Palmério, B., Rosenblum, J.P. and Stoufflet, B. (1989). Euler calculations by upwind finite element methods and adaptive mesh algorithms, *Notes on Numerical Fluid Mechanics*, *26*, 138-156. Vieweg, Braunschweig.

[6] Désidéri, J.-A. and Hemker, P.W. (1990). Analysis of the convergence of iterative implicit and defect-correction algorithms for higher-order problems, INRIA Sophia-Antipolis, Valbonne, Rapport de Recherche 1200.

[7] Fézoui, L. and Stoufflet, B. (1989). A class of implicit upwind schemes for Euler simulations with unstructured grids, *J. Comput. Phys.*, *84*, 174-206.

[8] Godunov, S.K. (1959). Finite difference method for numerical computation of discontinuous solutions of the equations of fluid dynamics (Cornell Aeronautical Lab. Transl. from Russian), *Mat. Sbornik*, *47*, 271-306.

[9] Hackbusch, W. (1981). Bemerkungen zur iterierten Defektkorrektur und zu ihrer Kombination mit Mehrgitterverfahren, *Rev. Roum. Math. Pures Appl.*, *26*, 1319-1329.

[10] Hackbusch, W. (1985). *Multi-grid methods and applications*. Springer, Berlin.

[11] Hemker, P.W. (1984). Mixed defect correction iteration for the solution of a singular perturbation problem, *Computing Suppl.*, *5*, 123-145.

[12] Hemker, P.W. (1986). Defect correction and higher order schemes for the multi grid solution of the steady Euler equations, *Lecture Notes in Mathematics*, *1228*, 149-165. Springer, Berlin.

[13] Jameson, A. (1983). Solution of the Euler equations for two dimen-

sional transonic flow by a multigrid method, *Appl. Math. Comput.*, *13*, 327-355.

[14] Koren, B. (1988). Defect correction and multigrid for an efficient and accurate computation of airfoil flows, *J. Comput. Phys.*, *77*, 183-206.

[15] Koren, B. (1990). Multigrid and defect correction for the steady Navier-Stokes equations, *J. Comput. Phys.*, *87*, 25-46.

[16] Lallemand, M.-H. (1990). Dissipative properties of Runge-Kutta schemes with upwind spatial approximation for the Euler equations, INRIA Sophia-Antipolis, Valbonne, Rapport de Recherche 1179.

[17] Lallemand, M.-H. and Dervieux, A. (1988). A multigrid finite element method for solving the two-dimensional Euler equations, *Lecture Notes in Pure and Applied Mathematics*, *110*, 337-363. Marcel Dekker, New York.

[18] Lallemand, M.-H. and Koren, B. (submitted). Iterative defect correction and multigrid accelerated explicit time stepping schemes for the steady Euler equations.

[19] Van Leer, B. (1979). Towards the ultimate conservative difference scheme V. A second-order sequel to Godunov's method, *J. Comput. Phys.*, *32*, 101-136.

[20] Osher, S. and Solomon, F. (1982). Upwind-difference schemes for hyperbolic systems of conservation laws, *Math. Comput.*, *38*, 339-374.

[21] Rizzi, A. and Viviand, H. (1981). Numerical methods for the computation of inviscid transonic flows with shock waves, *Notes on Numerical Fluid Mechanics*, *3*. Vieweg, Braunschweig.

[22] Roe, P.L. (1981). Approximate Riemann solvers, parameter vectors and difference schemes, *J. Comput. Phys.*, *43*, 357-372.

[23] Rostand, P. and Stoufflet, B. (1989). TVD schemes to compute compressible viscous flows on unstructured meshes, *Notes on Numerical Fluid Mechanics*, *24*, 510-520. Vieweg, Braunschweig.